Biogenesis of Landscapes: Insights from Calcium and Strontium Isotopes.

Thesis submitted in accordance with the requirements of the University of Adelaide for an Honours Degree in Geology

Jonathan James Schneider
November 2017

THE UNIVERSITY of ADELAIDE

BIOGENESIS OF LANDSCAPES: INSIGHTS FROM CALCIUM AND STRONTIUM ISOTOPES

BIOGENESIS OF LANDSCAPES

ABSTRACT:

Previous studies conducted at the Chillinup Nature Reserve (host to Lake Chillinup in southwestern WA) revealed the interconnected relationship between Eucalyptus lateral roots and clay pods hosted within its rooting zone. This bio-geological relationship between lateral roots and clay pods hosted within quartzitic sand dune, poses the problem of how Fe and Al rich soil pod structures could be formed from the percolation of freshwater through regolith depleted in such elements. It has been argued whether these clay pod structures have been produced by *inorganic* or via *biological* processes, where the former would involve chemical leaching of elements from top soils and their accumulation at deeper depths (i.e., pod sites). Alternatively, the biological origin (i.e., phytotarium concept) involves hydraulic uplift of Fe and Al by eucalyptus trees and their subsequent release via roots at sites of pods formation.
In this study, we applied elemental and isotope analyses on clay pods, soils, waters and eucalyptus organic tissues. Specifically, we used novel Ca and Sr isotopic proxies ($^{87}Sr/^{86}Sr$ and $\delta^{44}Ca$) coupled with elemental mobility profiles (tau (τ) normalised elemental profiles) with the impetus to confirm the source(s) of material for the formation and origin of the clay pods at the Lake Chillinup site. Our Ca and Sr isotope constraints revealed that eucalyptus trees access their nutrients and water sources primarily from a perched freshwater reservoir within the shallower soils above the deeper saline groundwaters. In addition, the tau-normalised profiles confirmed systematic leaching of all analysed elements (i.e., alkali earth metals and transition metals) from the top acidic soil, with subsequent enrichments of Al, Fe, Cr and Ge within the pod horizon (~10 to 50 cm depths), followed by local enrichments of Ca and Sr in deeper and more alkaline soils, below the pod horizons (~100 cm) where calcareous soils and structures were also observed.
Importantly, our $^{87}Sr/^{86}Sr$ and $\delta^{44}Ca$ data confirmed that alkali earth metals, such as Ca and Sr, in the studied clay pods originate from the local *inorganic* mineral sources, and our results do not support the biogenic origin of Ca and Sr in pod structures. However, these conclusions might not be directly applicable to the origin of Fe and Al in soil pods, as these major elements may still be sourced from deeper soils via hydraulic uplift mediated by eucalyptus trees. Overall, this study contributes the growing database of Ca and Sr isotope measuremnets from the earth's surface environments and terrestrial ecosystems, with implications for the global Ca and Sr biogeochemical cycles.

Keywords

Biogenesis, Soils, Clay Pods, Calcium, Strontium, Isotopes, Biogeochemistry, Eucalyptus

TABLE OF CONTENTS

LIST OF FIGURES AND TABLES

1. INTRODUCTION

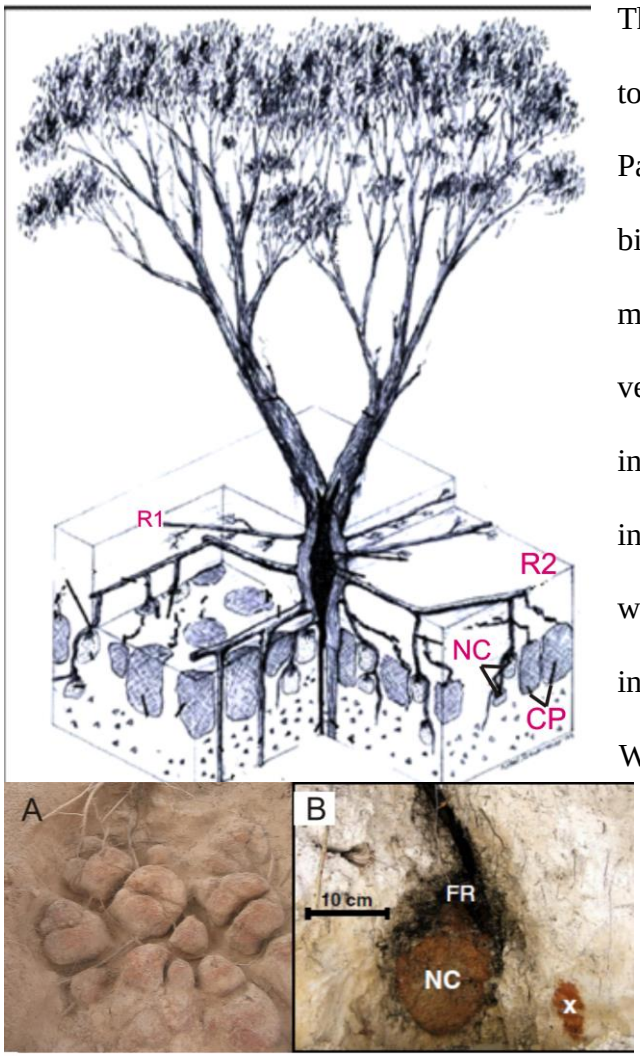

Fig. 1: (TOP) Rooting morphology of Eucalyptus.Incrassata studied at Chillinup Nature Reserve (WA). R1 superficial lateral root penetrates depths close to the surface. R2 lateral root with two classes of sinker roots in touch newly forming pods (NC) or deep sources of ground water. Mature Pods (CP) show traces of presumed root line. (A)Exposed horizon of individual pods within rooting zone of *Eucalyptus Incrassata* lateral roots. (Photo: W. Verboom). (B) Newly forming pod (NC) connected to lateral roots via fine rootlets (FR) next to embryotic stage of formation (X) (figure modified from Verboom and Pate (2013))

The impetus for this study is attributed to the pioneering work of (Verboom & Pate, 2006a, 2006b) who suggested that biological mutualism between soil microbes and various high order native vegetation (i.e., Eucalyptus trees) is involved in the bioengineering of soils in the semi-arid environments of south west Australia. Specifically, investigations at Lake King (2006) (in WA) unveiled a continuous soil horizon between *myrtaceous* (*eucalyptus*-dominated) and proteaceous (shrubs-dominated) vegetation zones. *Eucalyptus*, a major genus within the *Myrtaceous* family has been observed at Lake King and other semi-arid sites to host clay rich pod structures in close proximity to downward penetrating tap roots (see fig.1). It is suggested that after prolonged periods of formation, isolated pods coalesce with surrounding pods to form a mature pavement (Fig. 3). An extreme suggestion of

pavement formation is the utilisation of material by plants and/or associated microbes by mobilising them into a shallow pod horizon as means to sequester nutrients when required. It is proposed that such mutualism would additionally compete with other local flora attempting to tap into the same ground water and nutrient supply (Pate, Verboom, & Galloway, 2001). Such a relationship was considered to be indicative of the proposed 'phytotarium' concept and complements Darwin's theory of survival of the fittest (Verboom & Pate, 2006a). The Phytotarium concept suggests high order plants associated with mycorrhizal bacteria progressively modify regolith landscape in means for niche construction (i.e., biogenesis of landscapes). Biology and land plants thus play a fundamental role in shaping the soil chemistry and mineral weathering (Mareschal, Turpault, Bonnaud, & Ranger, 2013), however, it has always been a challenge to accurately qualify these effects and rates of plant-controlled manipulation, due to complexities related to the previous history of soil formation at specific sites (Berner, Berner, & Moulton, 2003). Inorganic clay aggregates are common in soil profiles and bridge the divide between organic and regolith bound elements facilitating cation exchange, an essential component for plant growth (Barré, Berger, & Velde, 2009).

Elemental cycling between global spheres and the phytotarium theory is enveloped within the broad definition of the of the Critical Zone (Brantley, Goldhaber, & Ragnarsdottir, 2007). The Critical Zone (CZ) groups biogeochemical cycling of elements within a weathering profile and above ground vegetation, spaning from the outer reaches of tree canopy down to the lower limits of the groundwater (Fig 2).

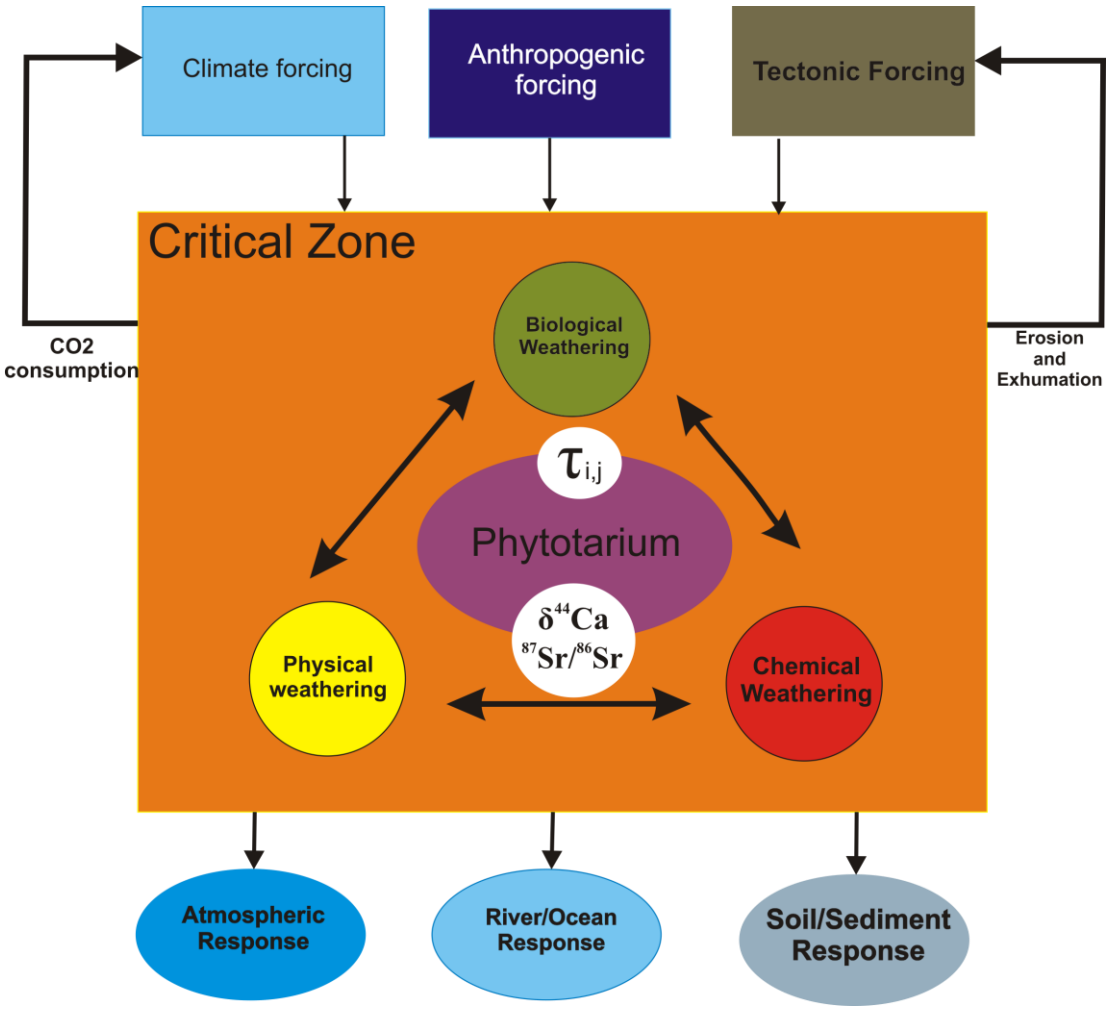

Fig 2: Coupling of chemical, physical and biological weathering within the Critical Zone (CZ). The phytotarium exists within bounds of the critical zone. Geochemical tools are used to constrain parameters of the phytotarium while linking data to the global scale (Reproduced from: (Brantley et al., 2007))

1.1 Study site

Lake Chillinup is a locality 250 km southwest of Lake King that exhibits such soil pavements (Fig. 4), and thus is ideally suited to farther evaluate the validity of the phytotarium concept in the formation of clay pavements (Pate & Verboom, 2009; Verboom, Pate, & Aspandiar, 2010). Importantly, the Lake Chillinup site has a road clearing cross cutting a dune system revealing the progressive development of clay

horizon and pods with respect to the local vegetation boundaries (Fig. 3). This unimpeded view on the development of clay pods provided the catalyst for further field research at this site which was completed in May 2017.

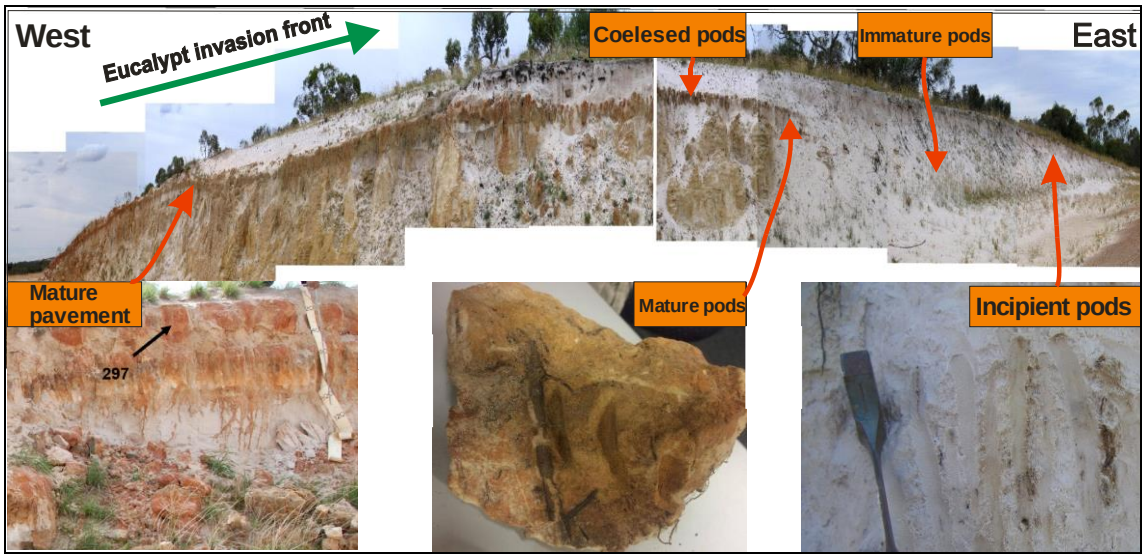

Fig 3: Progressive developmental stages of pod formation within transect of dune system at Lake Chillinup site (WA). Road construction allows for this unimpeded view of the soil profile. (Photos: W. Verboom)

The Lake Chillinup site, with a recent dune system, provides a unique natural laboratory (not affected by previous soil formation events) to study the formation of soil pods and horizons and the associated isotope biogeochemical cycles. This is because the local and geologically young (Quaternary) dune system composed of nutrient deficient quarzitic sand host sediment, lacks previous cycles of soil formation. As such, any input material required for the neoformation of clay pods can be traced using isotope proxies, which in turn will allow to constrain the sources of elements for the clay formation. These might include purely inorganic processes such as leaching of elements from the top soils and their accumulation in deeper depth where the pods are documented, or alternatively the biological 'uplift' of elements from groundwaters via plant roots (Barré et al., 2009;

Lucas, 2001) and their selective release at clay pod sites (i.e., phytotarium concept)

(Pate & Verboom, 2009; Verboom & Pate, 2006a, 2006b; Verboom et al., 2010)

1.2 Research objectives

This study uncovers the sources and bio-geochemical pathways of selected elements responsible for the formation of soil pavements and clay pods at the Lake Chillinup site Specifically, we use normalised elemental ratios (tau-values, τ) and stable calcium ($\delta^{44}Ca$) and radiogenic strontium ($^{87}Sr/^{86}Sr$) isotopes to further constrain the local elemental cycling and origin of these elements in the soil clay pods and pavements. Ultimately, this study aims to differentiate between the inorganic (i.e., mineral-derived) versus biological (i.e., plant-mediated) processes and their role in the constructions of soil pavements and pods genesis. This novel isotope approach will comment on the validity of phytotarium concept, and the role of inorganic and biological processes resulting in the genesis of clay pods and horizons within soil colonised by Eucalyptus trees. Overall, finding of this research will provide insights and information relevant to soil formation processes, ecosystem studies and agriculture.

From the isotope perspective, this paper contributes to the growing, yet still limited, database of stable Ca isotope measurements ($\delta^{44}/^{40}Ca$ variations) in the Earth's surface environments (Fantle & Tipper, 2014). The acquired data further refines our understanding of the global Ca biogeochemical cycle including the atmosphere, hydrosphere, biosphere and lithosphere reservoirs, and the associated geochemical pathways of Ca in a rock-soil-plant-water system.

2. HYDROGEOLOGICAL SETTING AND LOCAL VEGETATION

The Chillinup Nature Reserve is host to hypersaline playa lake, Lake Chillinup, in the Kalgan catchment located 5 km south of the Stirling Ranges, Western Australia (S34º32.54' E118º04.12')(Fig.4). Previous geological and geomorphological research of this area identified several quarzitic sand dunes radiating out from the eastern shore believed to have formed by north-west prevailing winds in periods of aridity in the late stages of the Pleistocene (Bowler, 1976; Pate & Verboom, 2009). A road cutting through the sand dune south LC revealed a transect promoting progressive genesis of a clay pods into a mature clay pavement (Fig. 3). Mineralogical observation of the sampled clay pods determined the presence of illite in dispersed with finer grained hematite (Chittleborough, 2017). It was clear from the lack of pelletisation that clay material was not emplaced by wind action but was formed in-situ via inorganic and/or biogenic processes (Verboom et al., 2010).

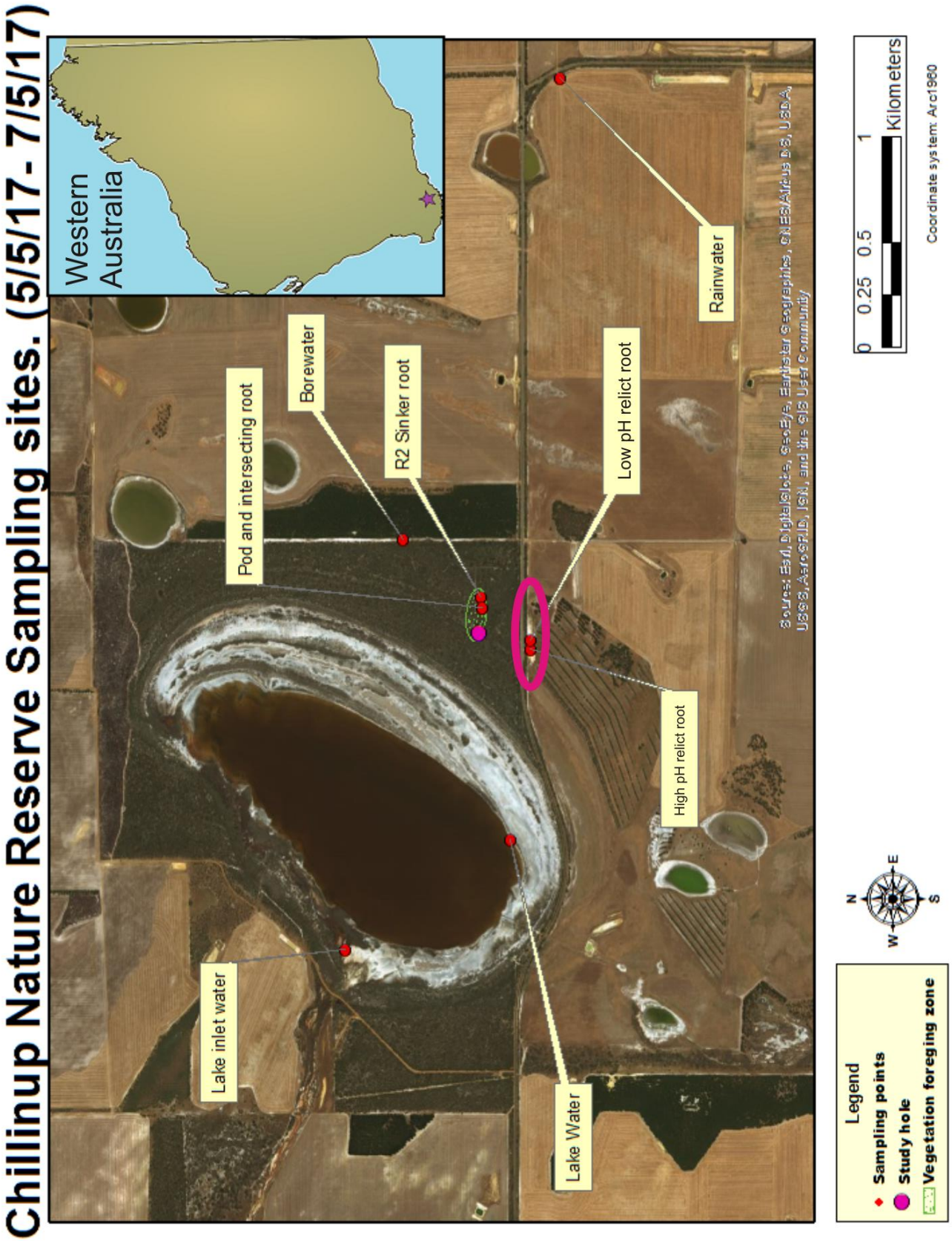

Fig 4: Regional extent of the Chillinup Nature Reserve (CNR) study area. Pink oval is dune road cutting depicting continuous horizon from newly formed pods to mature pavement. (Inset) Location of CNR in southern part of WA. (Figure modified from ESRI basemap

2.1 Local Vegetation

The lake Chillinup site is host to a mix of *Myrtaceous* and *Proteaceous* heath (shrubland), however much of the surrounding land has been cleared for pasture leaving only a few dunes fostering native plants and vegetation (Fig. 5). The species of interest in the reserve are: *Eucalyptus Incrassata* and *Eucalyptus Occidentalis* (Yate) which are presumed to have colonized local dunes and lunettes about 10’000 years ago (Verboom et al., 2010). Zones A and B, in fig 5, are defined by low growing shrubs and grasses inhabiting superficial pavements formed by the *Eucalyptus Occidentalis* (Yate). An immediate change in the dominant species of local vegetation can been seen in Zones B and C, which is aligns with the superficial clay pavements and the extent of Yate (Fig. 5C). The rooting morphology of the *Eucalyptus Incrassata* specimen, described in detail by Verboom et al. (2010), inhabits a region of open woodland interspaced by *myrtaceous* and *proteaceous* heath of zone C.

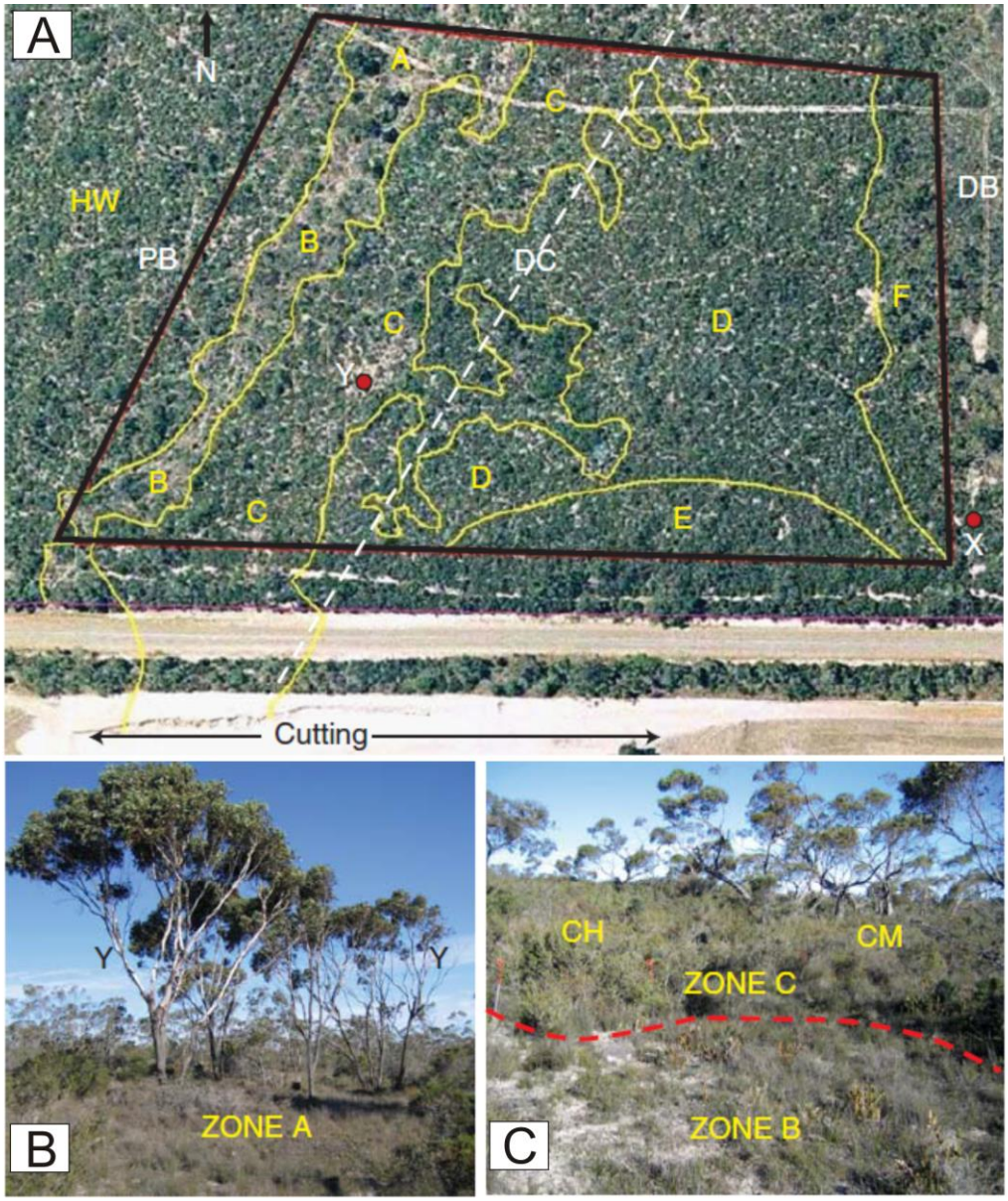

Fig 5: Vegetation zones defined within the lake Chillinup site.
(A) Extent of research area illustrating the primary zones (A-F) over the crest of quarzitic sand dune (DC). A diffuse boundary is between Zone A and B. Presence of *Eucalyptus Occidentalis* differentiates between A and B, as both zones exhibit shallow clay pods (10cm depth) and sparse ground coverage. (B) Yate groves (Y) associated with sparse understorey. (C) Sharp change of vegetation between Zone B and C. Sparse vegetation coverage aligns with the extent of superficial pavement. Zone C consists of a mix between *eucalyptus* woodland (CM) and *mytaceous:proteaceous* heath (CH). Zones D-F are not relevant for our study (Modified from Pate and Verboom (2009))

2.2. Eucalyptus Root/Pod Architecture

The occurrences and associations of the root system of *Eucalyptus Incrassata* and *Eucalyptus Occidentalis* (Yate), with respect to clay pods is apparent within fig 6. The 200-300 year old *Incrassata* selected for study by Verboom et al. (2010), bore two classes of lateral roots. R1 roots radiated from trunk 8-12m in superficial depths of about 10-30 cm. Unlike R1 laterals, R2 laterals had developed taproots connecting fine branch rootlets to newly forming pods. R2 laterals bore sinker roots that are able to sequester in horizons below clay pavements.

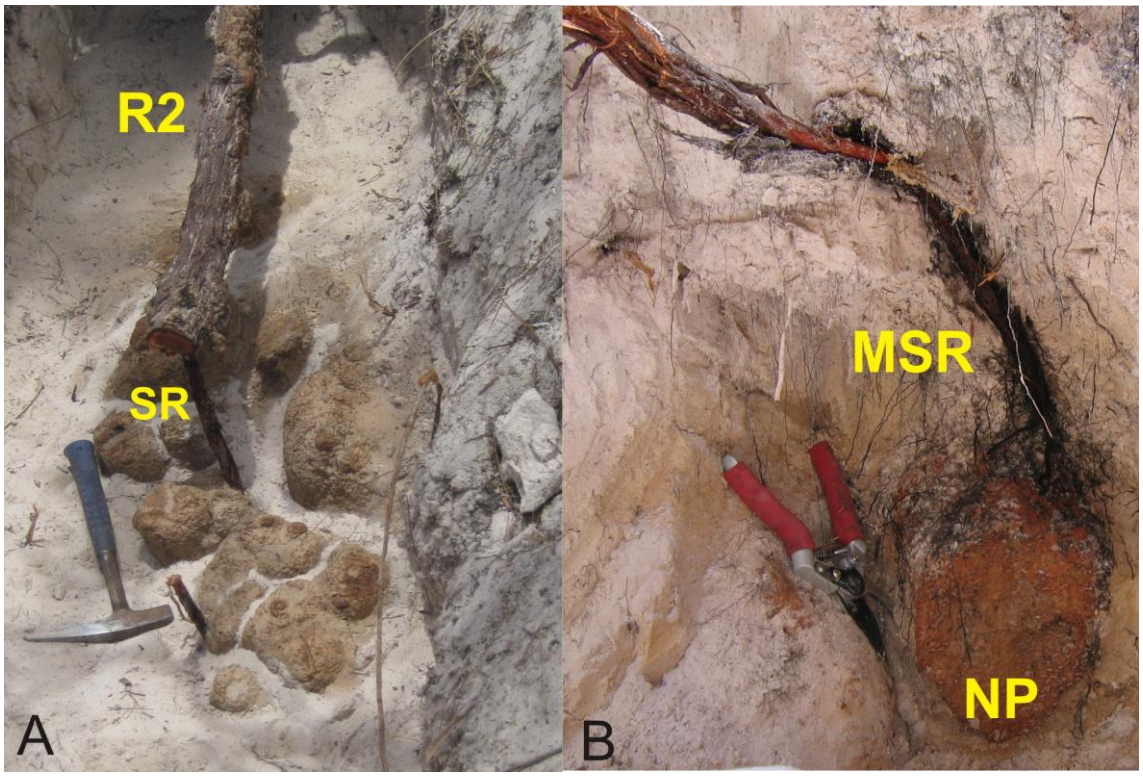

Fig 6: Spatial relationships between Eucalytus sinker roots and clay pods. (A) R2 lateral root facilitating sinker roots (SR) tapping into deeper water sources. (B) Mini sinker root attenuating from R2 lateral (not shown) into newly forming pod (NP) (Photo credit: W. Verboom)

2.3 Progressive Genesis of Clay Pods and Pavements at Study Site

Close association between clay pods and *Eucalyptus* is made increasingly apparent from the road cutting (see fig 4 for location). This site provided a fully exposed transect previously colonised and maintained by plants within respected zones of vegetation (fig.5A). Relict roots were seen to extend down to 9 m depth near the dune base, which is underlain by paleo-lake deposit. This road cutting also uncovered vertical transects through the dune (see lines 1 to 7, in Fig. 7) representing various stages of clay pods formation and extent of *eucalyptus* influence. Importantly, the constructed soil pH profiles suggest significant changes across the dune with more acidic conditions above the clay pavements and in early pod development, while more alkaline pH conditions were documented below developed pavements (Verboom & Pate, 2013; Verboom et al., 2010). Elemental analysis of a profile under *eucalyptus* through clay pod horizon indicated the enrichment of Aluminium and Iron in pod horizon. Verboom et al. (2010) assumed that acquisition of material for pod construction was largely sequestered by deeply penetrating tap roots tapping water sources proximal to lake sediment. Elements would travel upward through the xylem of tap root before released at sites of pod formation. In the summer months, when trees were likely to absorb nutrients from deeper horizons proximal to paleolake sediments, xylem sap extracted from lateral roots were found to be 100 times more concentrated in aluminium and five times concentrated in iron than in winter thus promoting biological uptake and redistribution through (Verboom & Pate, 2013; Verboom et al., 2010)

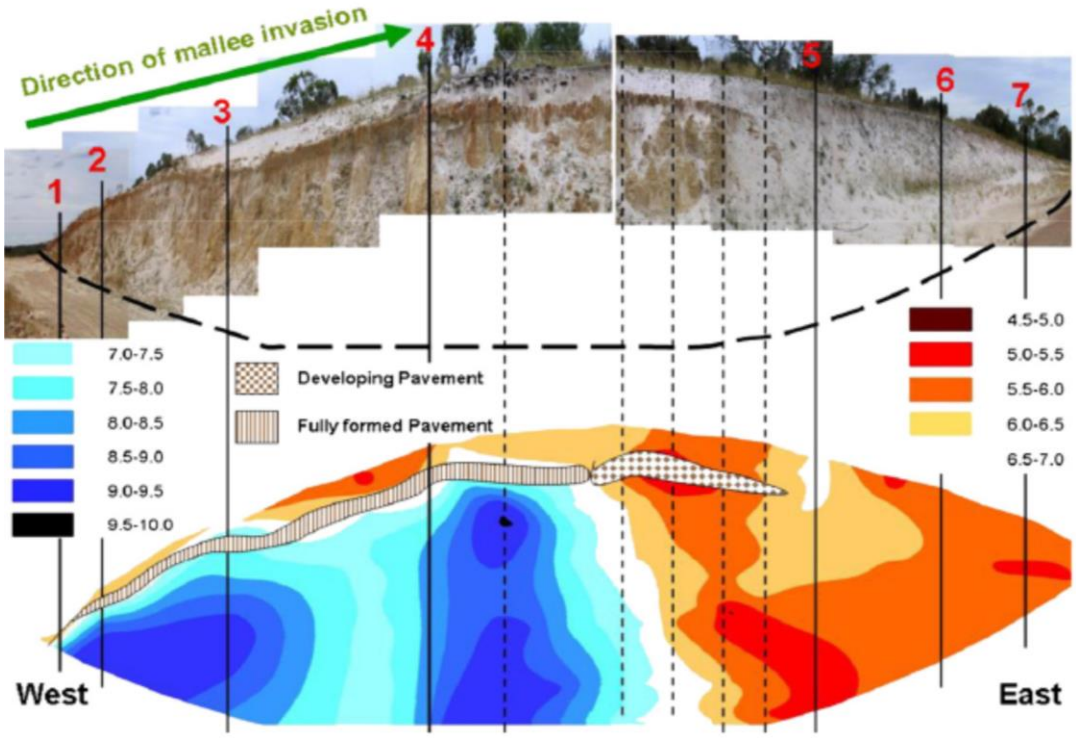

Fig 7: Progressive development of clay pavements associated with invading *Eucalypts* species , and the measured soil pH changes across the dune and their relationships with respect to clay pods and pavements formation.

3. ALKALINE EARTH METALS ISOTOPE PROXIES: CALCIUM AND STRONTIUM

3.1. Stable Calcium Isotope Tracer ($\delta^{44/40}Ca$)

Calcium (Ca) is a highly soluble alkali earth metal, which is also a major base cation and an essential nutrient for higher plants (Schmitt, Gangloff, Labolle, Chabaux, & Stille, 2017). There are six stable isotopes of calcium (^{40}Ca, ^{42}Ca, ^{43}Ca, ^{44}Ca, ^{46}Ca and ^{49}Ca) of which the isotopically lighter are kinetically favoured for absorption by

organisms and biological processes, which in turn leaves the residual calcium in soils and waters enriched in heavier isotopes (Farkaš, Déjeant, Novák, & Jacobsen, 2011). The natural variability of Ca isotopes is expressed as delta notation ($\delta^{44/40}$Ca values), in per mil (‰), relative to standard (for details see also the Method section). Overall, in the Earth's surface environments, there is more than 4 per mil variability in $\delta^{44/40}$Ca of various inorganic and biological Ca reservoirs and pools (see Fig. 8). The biologically complex Ca in plants and vegetation carries the isotopically lightest signatures, along with biological/skeletal carbonates, while the heaviest Ca isotope signatures are found in soil waters and particularly in seawater, from which large quantities of Ca are removed via biological uptake and biomineralisation.(Fantle & Tipper, 2014)

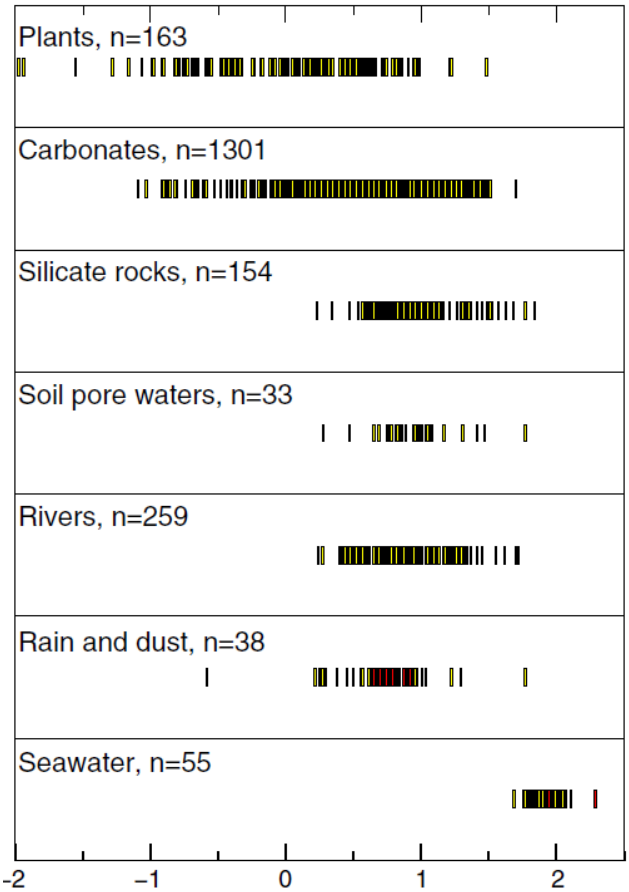

Figure 8: A compilation of δ^{44}Ca (‰, relative to NIST 915a) values in major Ca reservoirs on Earth, including silicate and carbonate rocks, waters, soils and plants (Fantle & Tipper, 2014)

3.2. Radiogenic Strontium Isotope Tracer ($^{87}Sr/^{86}Sr$)

Strontium (Sr), with a similar ionic radius and charge as Ca, has five naturally occurring isotopes (^{84}Sr, ^{86}Sr, ^{87}Sr and ^{88}Sr), where ^{87}Sr is also a product of radioactive decay of rubidium: ^{87}Rb. Due to the incompatible nature of Rb (compared to Sr or Ca), which is preferentially incorporated into melts, the continental crust carries more radiogenic ^{87}Sr due to decay of ^{87}Rb. Typically, this is reflected when comparing Oceanic crust (low in Rb) and continental crust (high in Rb). Sr, unlike Ca, is unsusceptible to such biological fractionation therefore can be used in tandem with Ca to infer source of uptake (Farkaš et al., 2011; Graustein, 1989). The prevalence and physical properties of these isotopes allow for evaluation of nutrient cycles at local, regional and global scales(Halverson, Dudás, Maloof, & Bowring, 2007).

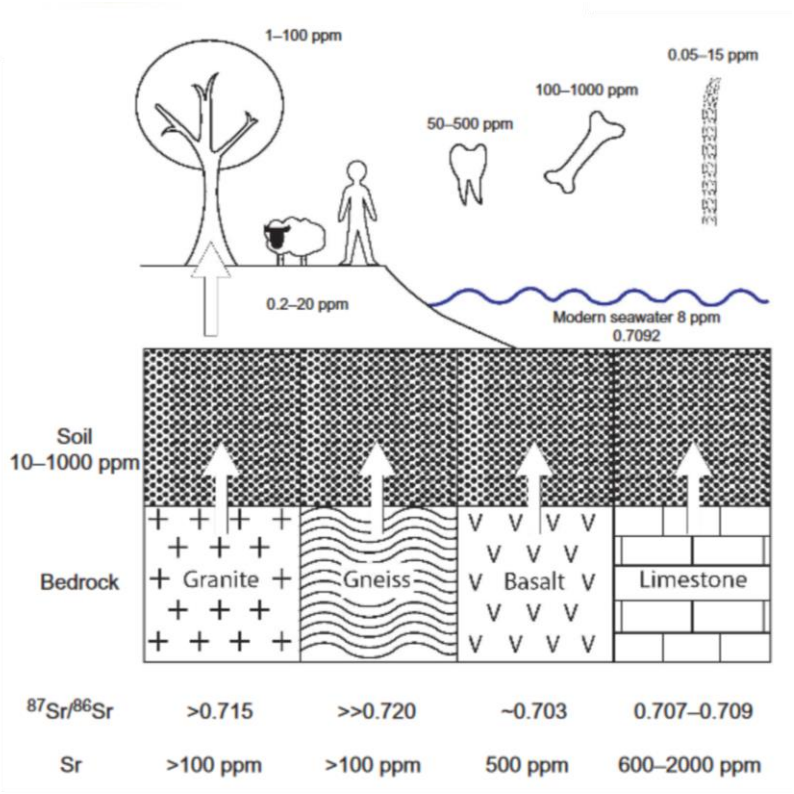

Figure 9: Sr concentrations and isotope compositions ($^{87}Sr/^{86}Sr$) of main lithologies and rock types, and the associated sediments are reflected in the modified sediments in which they produce. (Frei, 2012)

4. METHODS

This study utilised various methods and research techniques applied in the field, laboratory and, during geochemical and isotope analysis, which are all described in detail in the sections below.

4.1 **field methods and sample collection**

A suite of samples containing soils, waters and organic materials were collected at CNR at a Lake Chillinup site in May 2017. Organic materials include samples of *Eucalyptus* leaves, woody tissue and roots from two species: *E. incrassata and E. occidentalis.* A complete soil profile (from 0 to 200 cm, Fig. 12 and Table 1) was extracted from an area dominated by the growth of *E. occidentalis* with a sparse understorey that is indicative of the presence of clay pavements in the soil profile (Table 1). In addition, a complete pod cross-section with the enclosed roots of *E. incrassata* was sampled during one of the previous excursions at this site (Verboom et al., 2010). Root like geologic structures (i.e., relict roots channels, Fig. 11) were collected from both acidic and alkali regions of the road cutting. Finally, water samples including rainwater, lake water and local groundwater (from a depth of ~350 cm) were also sampled at the Lake Chillinup site.

Table 1: Number of samples collected per category. Location of samples are found within Fig 4.

Category	Sample	Number of Samples
Eucalyptus Incrassata	Leaves	1
	Woody Tissue	1
	R2 Root (intersecting pod cross section)	1
	R2 Root	1
Eucalyptus Occidentalis (Yate)	Leaves	1
	Woody Tissue	1
Soil	Yate soil profile (0-200cm)	8
	Pod cross section (root to rim)	3
study dune	Developmental stages of clay pod/pavement	6
	Trace root (Low pH)	1
	Trace root (High pH)	1
Water	Lake inlet	1
	Lake	1
	Ground water (350cm)	1
	Atmospheric deposition	1

4.2 Chemical Preparation of Samples

Collected samples were prepared for the elemental concentration and Ca and Sr isotope analyses performed via ICP-MS and TIMS instruments, respectively.

4.2.1 Organic Materials

Leaves, roots and woody tissues were weighed and ashed in 30 ml-volume Nickel crucibles at 450 ^{o}C for 4 hours. Once ashed, a dry weight was recorded and ashed samples were digested in 7M HNO_3 to oxidise any organic residue that may affect ICP-MS and TIMS measurements. Sample solutions with ashed and dissolved organic materials were evaporated and redissolved in 2% HNO_3 for ICP-MS. An aliquot of sample solution containing approximately 1 ug of Sr was weighed and prepared for chemical purification of Sr via prepFAST-MC system, using 2M HNO_3 as working acid, following the procedure of Romaniello et al. (2015).

4.2.2 Soil Samples, Clay Pods and Calcareous Roots

The soil profile, pod and root structures from the study dune were weighed and dissolved in a mixture of concentrated HNO_3 and HF acids following standard clean lab procedure for silicate dissolution. Acid digested samples were evaporated and redissolved in 2% HNO_3 for ICP-MS. An aliquot of sample solution containing approximately 1 ug of Sr was weighed and prepared for chemical purification via prepFAST-MC system.

Calcareous root structures strongly reacted with Hydrochloric acid (HCl), and these materials were thus dissolved in 2M HCl at room temperatures over 1 day. The sample was dried and redissolved in 6M HCl and left for an additional day. Second digestion confirmed an outer calcareous layer surrounding an internal possible siliceous structure that remained undissolved. Ashing of these residual material confirmed no significant presence of woody tissues. This sample was thus separated into an undissolved siliceous internal structure and a leachate (i.e., calcareous phase). The internal structure was digested following the procedure for soils (i.e., a mixture of HNO_3 and HF), and the calcareous phase was digested in HCl.

4.2.3 Water Samples

Four water samples collected (see Table 1) underwent filtration using a syringe with 0.45 um filter tip. The hypersaline nature of the lake inlet and lake water samples required dilutions of 60 and 100 times, respectively.

4.3 Elemental and Isotope Analyses

4.3.1 ICP-MS Analysis

Elemental concentrations were determined by the Ailgent 8900 ICP MS (QQQ) at the University of Adelaide. Elements selected for the analysis include: Calcium (Ca), Strontium (Sr), Potassium (K), Iron (Fe), Sodium (Na), Magnesium (Mg), Germanium (Ge), Aluminium (Al), Zirconium (Zr), Chromium (Cr), Barium (Ba), Sulphur (S), Phosphorus (P) and Cerium (Ce). A certified rock standard BCR-2 was measured and monitored throughout elemental analysis to ensure reproducibility and validity of our concentration analysis, which has a typical error of about 3%.

4.3.2 Chemical Purification of Sr via PrepFAST

The separation of Sr from a sample matrix, prior to the isotope analysis, was accomplished using the semi-automated PrepFAST-MC system at the University of Adelaide, following the procedure of Romaniello et al. (2015). Briefly, volume of each sample was weighed out from stock solutions (2M HNO3) to yield ~1µg of Sr, which was processed via PrepFAST. Limits of 500µg Ca to 1µg Sr was maintained to minimize the effects of Ca overload on column, thus maximising the yield of separated Sr (Romaniello et al., 2015). The separated Sr fraction was eluted into corresponding sample vial with 6ml of 2M HNO3, and a drop of 0.1 M phosphoric acid (H3PO4) was added to the solution prior to evaporation.. In the circumstance that after evaporation the remaining Sr and H3PO4 appeared opaque, a nominal 2ml of 15M nitric acid was added and a sample solution was left on hotplate at 140C overnight. This process facilitated oxidation of any organic material remaining after separation of Sr on PrepFAST, which may cause potential problems during the Sr isotopic analysis.

4.3.3 Strontium Isotope Analysis (87Sr/86Sr) by TIMS

The Sr isotope ratios were measured by TIMS Phoenix instrument at the University of Adelaide, with typical reproducibility on $^{87}Sr/^{86}Sr$ of less than 0.000005 (2SE), as determined by repeat measurements of standards and/or samples. Typically, around 600 ng of Sr was loaded onto Re-filament, and NIST SRM 987 standard was included for data quality control during the analysis of the samples.

4.3.4 Calcium Isotope Analysis ($\delta^{44}/^{40}Ca$) by TIMS

The stable Ca isotope compositions (i.e., $\delta^{44/40}Ca$ values) of soils, waters and vegetation samples were determined via TIMS, using a 'double spike' approach with a ^{43}Ca-^{42}Ca isotope tracer, following the methods described in Holmden and Belanger (2010) and Farkaš et al. (2016). Prior to the Ca isotope analysis all samples were mixed with double-spike and then passed through the cation exchange resin (cf., Holmden & Belanger, 2010), and the subsequent isotope analysis of purified Ca fractions were performed using a Thermo Triton TIMS instrument at the Saskatchewan Isotope Laboratory (University of Saskatchewan, Canada), with a typical 2SE reproducibility on $\delta^{44/40}Ca$ value of about 0.05 per mil (‰).

The $\delta^{44/40}Ca$ values reported in this study are normalised to modern seawater (IAPSO) standard, based on the following relationship:

$$\delta^{44/40}Ca\ (‰)_{\ IAPSO} = [(^{44}Ca/^{40}Ca_{\ sample}) / (^{44}Ca/^{40}Ca_{\ IAPSO}) - 1] * 1000 \qquad \text{(Eq. 1)}$$

4.4 Normalised Elemental Ratios (tau-values, τ) for Soil Research

The relative enrichments and depletions of elements in the regolith during soil formation, with respect to an unweathered bedrock, can be quantified using the mass-transport function (Eq. 2) or so-called tau-normalised elemental profiles (Brantley et al. (2007). Accordingly, the abundance of immobile elements such as Ti and/or Zr are used a reference for the tau-normalisation (τ), which corrects for volume contraction, expansion and any dilution or enrichment effects between multiple elements within a system during soil formation and biological processes. The tau-normalised values for specific element are calculated based on the following relationship (Brantley et al. (2007):

$$\tau_{i,j} = \left(\frac{(j_w * i_p)}{(j_p * i_w)}\right) - 1 \qquad \text{(Eq. 2)}$$

Where ***i*** = the concentration of immobile element (Ti or Zr), ***j*** = concentration of element of interest, ***w*** = concentration of element within weathered soil, and ***p*** = concentration of element within parent rock (i.e., unweathered bedrock). Briefly, τ values less than zero (i.e., negative values) indicate that an element of interest was leached and weathered from the soils (i.e., showing depletions relative to immobile

reference elements: Ti and/or Zr). In particular, τ values of -1 would indicate 100% loss or leaching of element from the soils compared to unweathered bedrock and/or source sediment (and τ of -0.5 would indicate 50% loss). In contrast, positive τ values above zero, indicates that the element of interest has been enriched or accumulated in the soil profile, either from external sources (e.g., atmospheric deposition) or that the element has been enriched in certain soil depths due to its leaching from top soils (i.e., depletion-enrichment profile). Finally, τ values equal zero indicates that the element has not been mobilised and/or accumulated in the soils, and thus behaves conservatively as our reference immobile elements Zr and Ti.

For this study and calculations of τ values for selected elements, we collected and analysed eight bulk soil samples from various depths (ranging from 0-10 cm to 190-200cm depth) along a single soil profile or soil pit (see Fig. 12), exposed at Lake Chillinup site. These samples thus represent a continuous transect across the organic top soils, clay pavements, and the deeper mineral soils.

5. RESULTS

5.1 Field Observations

Exploration of the CNR, and the Lake Chillinup site performed in early May 2017, revealed evidence of of past research and sampling at this site done by Verboom et al. Specifically, excavation by Verboom et al. (2010), and our own observations revealed *Eucalyptus Incrassata* rooting morphology that remained still exposed allowing for first hand observation of the intimate relationships between downward penetrating tap roots

and clay pods (Fig. 8A, B).

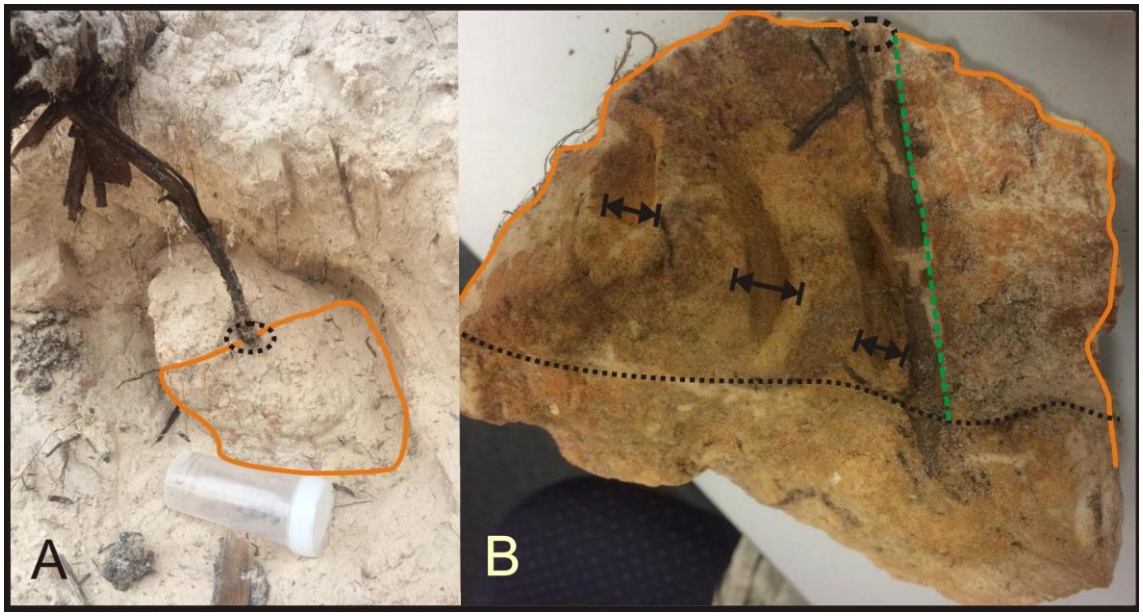

Fig 10: (A) R2 sinker root of *E.Incrassata* penetrating associated clay column. Defined is the outer extent that would be exposed to surface (orange) and point of intersection of root (dashed) (B) Cross section of pod illustrating 1cm sampling points from the imprint of root left after extraction (green).

Sampling campaign in late 2016 targeted different stages of pod genesis from newly forming incipient pods transitioning through to mature pavements (fig.12)

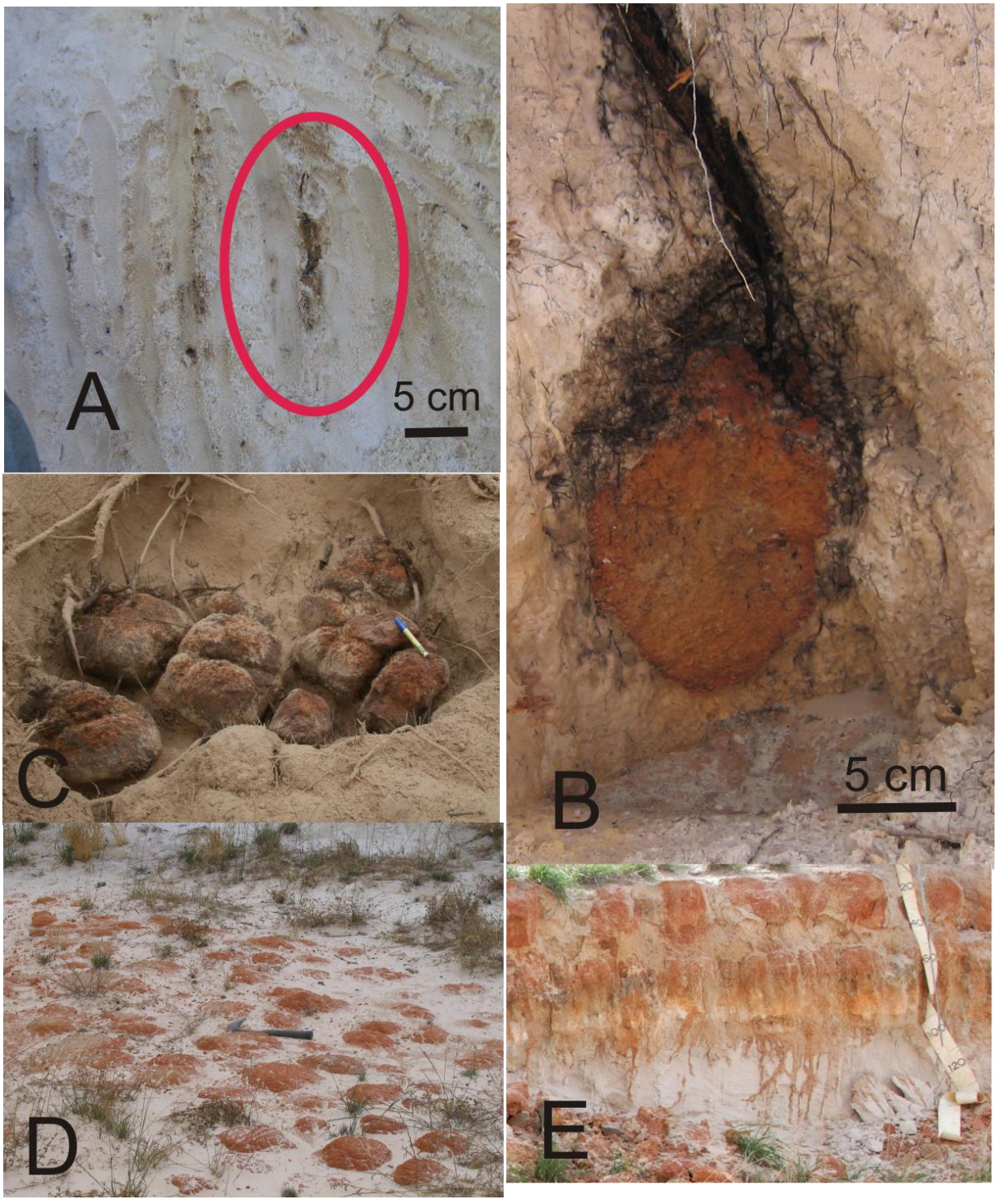

Fig 11: The developmental stages of clay pods observed at the Lake Chillinup site. (A) Embryotic stages of pod formation. (B) Immature pod attached to mini sinker root propagating from R2 lateral. (C) Mature pods in close proximity to lateral roots. This emphasises that pod platforms are not bedding plains typical of clay formation. (D) Increasingly coalesced Pods are observed on the

road cutting (E) Mature pavement formed by the progressive pod construction and subsequent coalescing in the Western reaches of the road cutting.

Ancestral Root channels were exposed from the cutting in both basic and acidic regions under clay horizon depths (Fig. 10). High pH regions of the cutting exposed intact traces of relict of calcareous ancestral roots. Application of Hydrochloric Acid (HCl) indicated presence of carbonate.

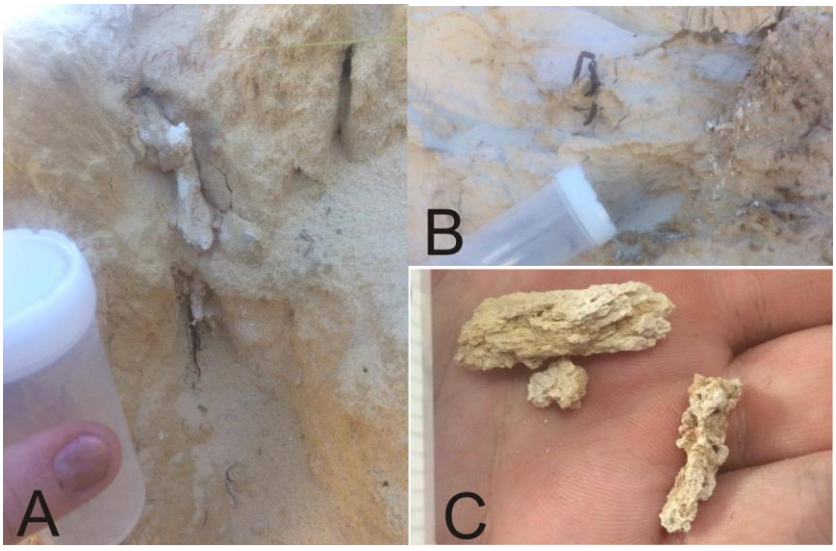

Fig 12: (A) Calcarious 'relict root' trace occurring within regions of high pH of the road cutting in fig. 8. (C) root traces were found concentrated within high relief tabular structures with in regions of low pH and unpavemented vertical profile. D) close view of low pH fragments.

5.2 Analytical Results - Elemental Concentration Data

This section refers to geochemical tools, i.e., tau-normalised elemental values ($\tau_{i,j}$) discussed in methods section to evaluate the relative elemental leaching and accumulation, to further constrain the sources and pathways of selected elements in along the soil profile and pods genesis at the Lake Chillinup site at the CNR.

5..2.1 Elemental Analysis and tau-normalised elemental profiles (τ-values)

The tau-normalised elemental profiles, calculated based on (Eq.1), quantify percentage loss or gain of an element across the soil profile with respect to unweathered regolith concentration. Titanium (Ti), as an immobile element reference, was used for the normalisation for all our calculations of tau-normalised element profiles (Fig.12).

As to alkaline earth metals, Ca and Sr tau-normalised profiles show both consistent trends as a function of the soil depths. At depths within the pod horizon (10-50cm) depletion of Ca and Sr in soil profile is greater than 75% (τ-value = -0.75). Leaching of Ca and Sr however decreases to about 50% in transition zone (at depth of ~75cm) and peaks at 60% enrichments (τ-value = +0.60) at depths of about 100-110 cm, indicating accumulation of Ca and Sr at these particular depths. Ba exhibits a similar trend as Ca and Sr albeit with smaller leaching rates, as well as enrichment effects, with the exception of a top soil. In contrast, Mg shows only detectable depletion profile, especially in the shallower soil depths (from 0 to ~100 cm). Overall, all studied alkali earth metals (Ca, Sr, Ba and Mg) show systematic depletions in shallower depth, and especially within the area of clay pods formation (10 to 50 cm).

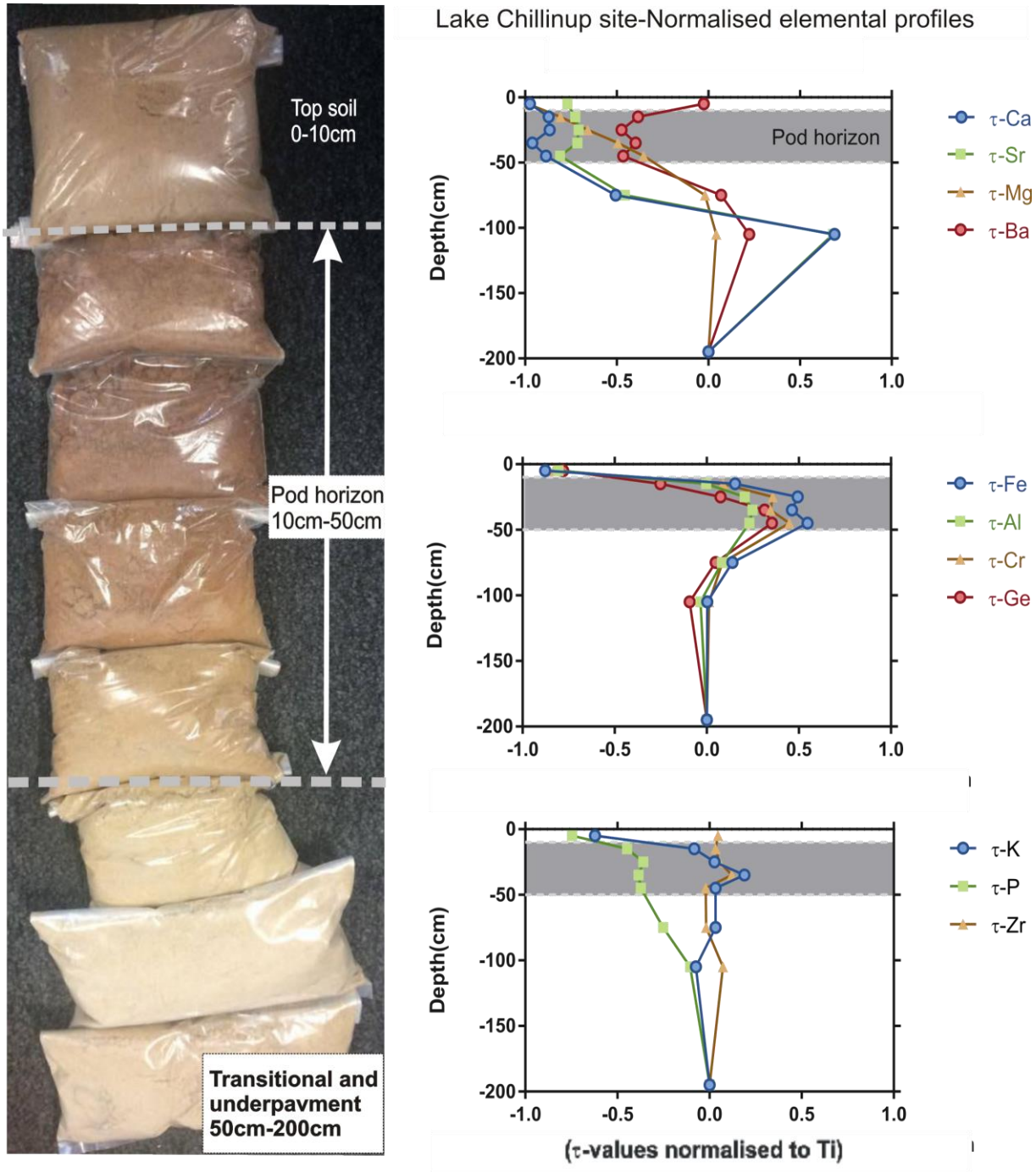

Fig 13: Normalised Elemental profiles of study hole on within Yate invaded Chillinup dune. (Left) Selceted depths within the dune; Top soil (0-10cm), Pod horizon (10cm-50cm), Transitional horizon (50cm-80cm) and underpavement (80cm-200cm) with the highest resolution targeting pod horizon depths (10cm-50cm) (Right, Top) The harmonic trends between Ca and Sr suggest accumulations at 105cm depth. (Right, Middle) Transition metals and Ge suggests to have leached and then accumulated within the 10-50cm depth of the profile which corresponds to depth range of podulisation. (right, Bottom) K is enriched within the pod horizon while P is more accumulated at depths.

As to transition metals (Fe, Cr and Al), these were also strongly leached from the top organic soils (showing up to 90% depletions), however, these elements show also significant enrichments (up to 50%) in deeper depths, especially within the clay pods horizon (see Fig. 12). As to Ge, which is main constituent of clay minerals, the tau-normalised Ge profile also show maximum enrichments within the pod horizon, in agreement with the prevalent occurrences of clays (i.e., clay pods) at these depths.

5.3 Analytical Results - Calcium and Strontium Isotope Data

The measured radiogenic Sr and stable Ca isotope variations in different sources and pools of these alkali earth metals (including soils, waters and organic materials) are discussed in detail in the sections below.

Our samples collected in May 2017, thus provide an 'isotopic snapshot' of the local biogeochemical cycles of Ca and Sr, which in turn allows to constrain the main sources of these elements for vegetation growth as well as the genesis of clay pods and horizons. It should be mentioned however that both Ca and Sr are only trace constituents in the clay pods and the major elements in these presumably bio-engineered soil structures are actually iron (Fe) and aluminium (Al), see Fig. 13. However, the latter is a mono-isotopic element (there is only one stable isotope of ^{27}Al), and the former is a redox-sensitive metal and thus isotope studies of Fe proved too problematic for source tracing. In contrast, both Ca and Sr are highly soluble and not redox sensitive elements, with multiple naturally occurring isotopes, which makes them ideally suited

for the isotope tracing of sources with implications for the ‘inorganic‘ versus ‘biogenic‘ origins of the studied clay pods.

5.3.1 Stable δ^{44}Ca variation at the Lake Chillinup Site

Isotopic variations of $\delta^{44/40}$Ca (or δ^{44}Ca) of different sources and pools of Ca at our study site are illustrated at Fig. 14.

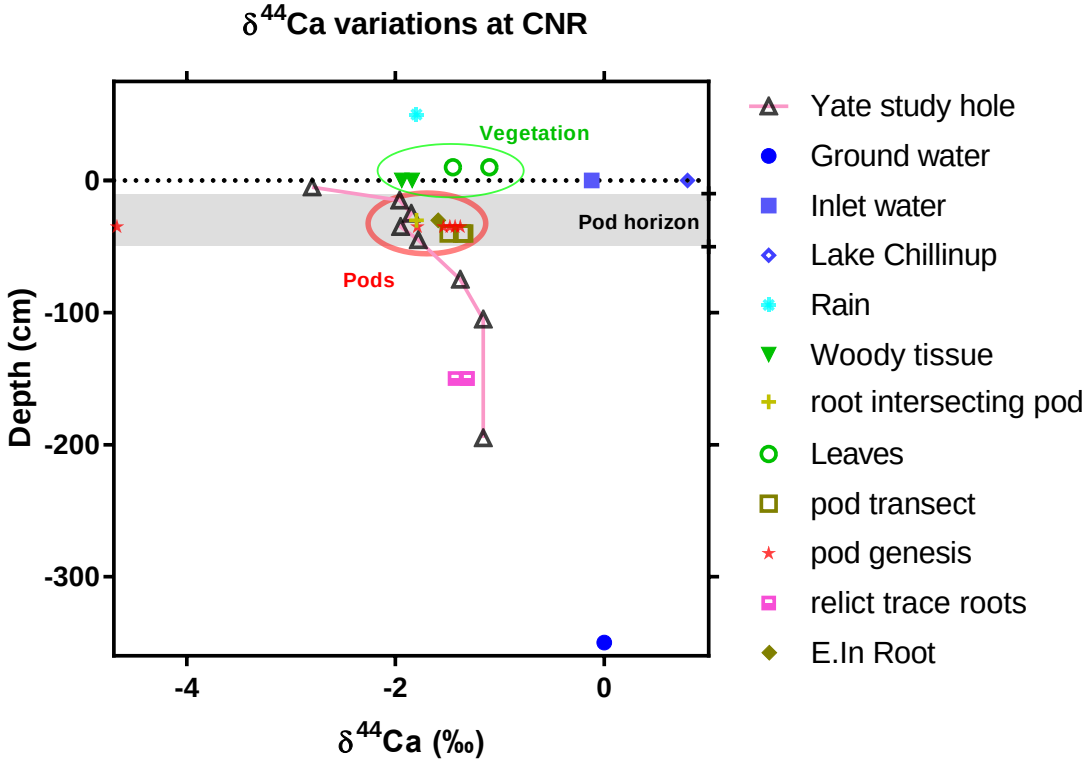

Figure 14: Variations in stable $\delta^{44/40}$Ca composition (in per mil relative to modern seawater – IAPSO) for different sources of inorganic and biological pools of Ca at the Lake Chillinup site. Specifically, these include ‘vegetation’ samples (Mixed eucalypt woody tissue, leaves and roots) and ‘pods’ (clay pod transect (fig. 8B), pod genesis, and pod horizons within Yate study hole).

Overall, we observed that vegetation and clay pods have similar δ^{44}Ca variations (scattering around -1.5‰), and overlapping also with the Ca isotope composition of local atmospheric deposition (i.e., rain with δ^{44}Ca of -1.8 ‰). In contrast, lake waters and ground water yielded systematically higher (i.e., heavier) δ^{44}Ca signatures up to

+0.8‰. The largest variations are however observed for the soil profile (0 to 200 cm depths), and these show systematically lower δ44Ca signatures at the top soil, and higher values at deeper depths (see Fig. 13).

5.3.2 Radiogenic $^{87}Sr/^{86}Sr$ variations at the Lake Chillinup Site

Isotopic variations of $^{87}Sr/^{86}Sr$ in various Sr pools and sources at our study site are shown in Fig. 15. Unlike Ca isotopes, which show similar $\delta^{44}Ca$ signatures for local vegetation and soil pods, the $^{87}Sr/^{86}Sr$ tracer revealed marked differences between Sr associated with pods (which have very radiogenic values of about 0.765) and organic material of local vegetation yielded low $^{87}Sr/^{86}Sr$ of about 0.712 (see Fig. 14). The Sr isotope composition of vegetation (woody tissues, leaves and roots) also overlaps with the $^{87}Sr/^{86}Sr$ of local water sources, including atmospheric deposition (rain), lake water and ground water which have values between ~0.710 and ~0.714. Similarly to Ca isotopes, the largest variations in $^{87}Sr/^{86}Sr$ is observed for the soil profile (0 to 200 cm, i.e., Yate study hole) which shows the most radiogenic values at the top soils and progressively less radiogenic signatures at deeper depths, with clay pods sitting between (Fig. 15).

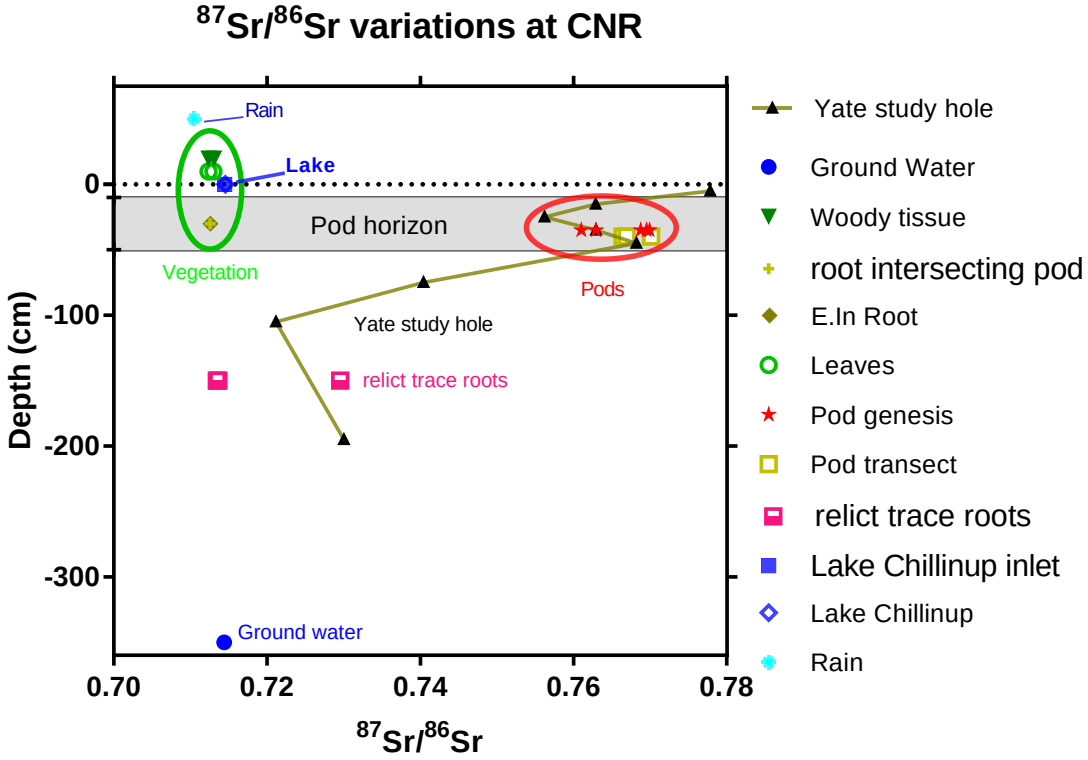

Fig 15: Variations of the radiogenic $^{87}Sr/^{86}Sr$ ratios in different sources and inorganic and biological Sr pools at the Lake Chillinup site, including waters, soils and vegetation.

Table 2: Isotopic values of Chillinup sampling suite

Sample	Sr (ppm)	87Sr/86Sr	2se	Ca (ppm)	d44Ca (‰ seawater)	2s.e.
Ground water	1.71	0.714418	0.000003	99.48	0.00	0.04
lake inlet	2.63	0.714478	0.000004	102.17	-0.12	0.03
lake	17.95	0.714585	0.000010	168.70	0.80	0.03
Rain	0.04	0.710496	0.000004	2.22	-1.80	0.06
Soil profile: H3 0-10	9.72	0.777829	0.000004	1166.79	-2.80	0.03
H3-10-20	21.26	0.762873	0.000003	2278.83	-1.96	0.03
H3 20-30	22.75	0.756190	0.000003	2353.06	-1.85	0.05
H3 30-40	21.70	0.762922	0.000004	2332.74	-1.95	0.03
H3 40-50	15.67	0.768175	0.000003	2214.21	-1.78	0.03
H3 70-80	34.02	0.740425	0.000003	5029.55	-1.38	0.04
H3 100-110	98.97	0.721164	0.000004	17556.14	-1.16	0.03
H3 190-200	57.90	0.730017	0.000003	9319.20	-1.16	0.03
E.Incrasata woody tissue	1493.64	0.712356	0.000004	8665.72	-1.94	0.04
E.Incrasata Leaves	511.69	0.712368	0.000003	4041.94	-1.45	0.03
E.Incrasata root intersecting (P1,2,3)	1943.56	0.712568	0.000003	8042.73	-1.80	0.04
E.Incrasta Root	1225.89	0.712625	0.000003	10864.09	-1.59	0.04
E.Occidentalis (Yate) Woody tissue	1090.71	0.713069	0.000003	7688.03	-1.84	0.03
E.Occidentalis (Yate) Leaves	472.66	0.713015	0.000004	5731.26	-1.10	0.02
P1 (pod transect root to rim)	15.68	0.766381	0.000004	2444.50	-1.36	0.04
P2 (pod transect root to rim)	13.90	0.766925	0.000004	347.20	-1.34	0.03
P3 (pod transect root to rim)	13.99	0.770092	0.000004	1795.62	-1.49	0.04
Pod Genesis- Initial	6.71	0.752350	0.000006	84.74	-4.67	0.03
PG- Immature	15.45	0.769523	0.000003	599.05	-1.38	0.04
PG- mature pods	13.42	0.769930	0.000004	392.96	-1.43	0.04
PG- Coelesced pods	22.84	0.768746	0.000003	868.30	-1.79	0.06
PG- Mature pavement (297)	11.99	0.762934	0.000004	537.97	-1.48	0.04
PG- Mature Pavement (299)	14.57	0.761015	0.000003	462.51	-1.54	0.05
Low pH trace root	10.01	0.729562	0.000003	1663.59	-1.43	0.03
High pH trace root	597.41	0.713448	0.000003	40084	-1.31	0.05

6. DISCUSSION

6.1 Tau-Normalised Elemental Trends Across Soil Profile

Elemental concentration data and the calculated tau-normalised profiles confirmed high degree of leaching in the acidic top soils (above the clay pods) for all elements investigated (i.e., alkaline earth metals, transitions metals, and selected nutrient

elements), with the exception of Ba and two immobile elements: Zr and Ti (see (Fig. 13). In contrast, at the depths where the clay pods become abundant (i.e., between 10 and 50 cm), we observed very different behaviour for different groups of elements. Specifically, all alkaline earth metals (Ca, Sr, Ba, Mg) showed significant depletions of about 40 to 90% at these depths (~10 to 50 cm), while Fe and Al and other transition metals are considerably enriched (between 20 to 50% gains) in the area of the clay pavements. This, in turn, suggests that these enriched elements such as Fe and Al are also major constituents of the clay pods structures, which is in agreement with previous studies (Verboom et al., 2013). At deeper depths below the clay pavements (i.e., below 50 cm) most of elements behave conservatively, approaching the composition of the least weathered sources, i.e., quartzitic sediments at depth of ~200 cm. The only exceptions are Sr and Ca (and partly Mg) as these elements exhibit enrichments at deeper depths (particularly at ~120 cm), which is likely related to the formation and accumulation of calcareous materials and $CaCO_3$ soils structures due to higher pH and more alkaline conditions at these depths (see also Figs. 12 and).

6.2 Calcium and Strontium: Tau-Normalised Profiles and Isotope Variations

Based on our tau-normalised data, it is obvious that the biogeochemical cycles of Ca and Sr within the studied soil profile are tightly coupled, as the calculated trends for these two elements are basically identical (see Fig. 13). Importantly, the observed depletions and enrichments of Ca across the soil profile (i.e., changes in τ-Ca with depths) are also closely linked to changes in the Ca isotope composition of the bulk sediments (see Fig. 16). In particular, the highly Ca-depleted top soils yielded the

isotopically lightest signature with $\delta^{44}Ca$ as low as -2.8‰, and the soils become progressively isotopically heavier with an increasing depth, reaching a value of -1.2‰ at depths of 100 to 200 cm.

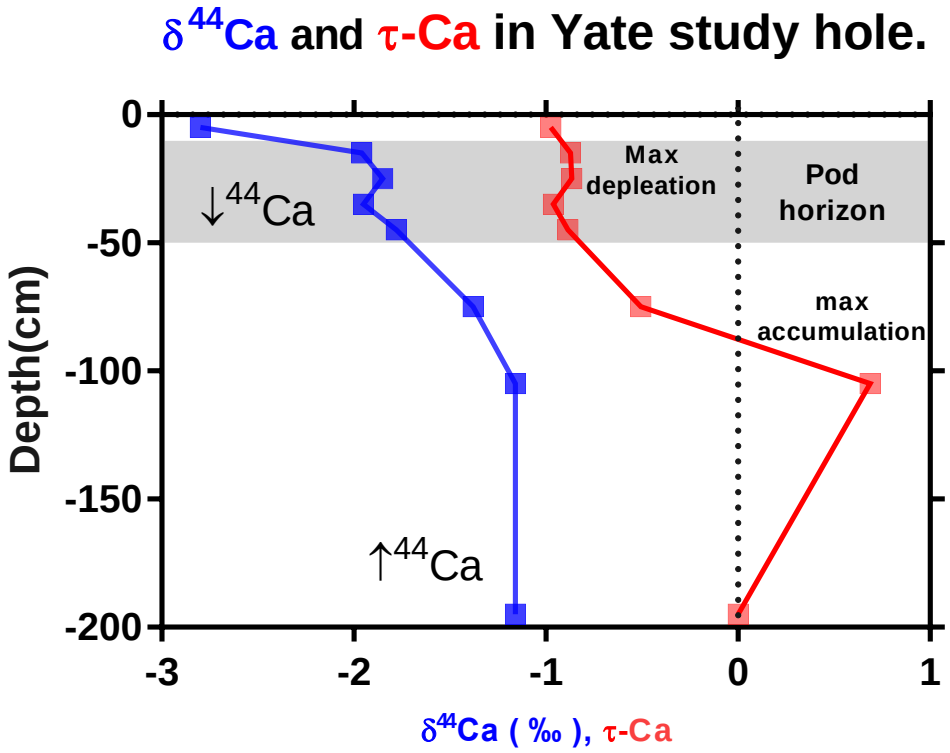

Fig 16. A comparison of the Ca mobility (i.e., enrichment/depletion patterns, or tau-values, red symbols) and the corresponding Ca isotopic variations (blue symbols) across the soil profile (Yate study hole) from the Lake Chillinup site.

Overall, these results suggest that Ca is readily leached in the low pH and acidic top soils, and during this process the heavy Ca isotopes seem to be preferentially released and mobilised from soils leaving behind the isotopically light Ca-depleted residuum. Such mobilisation and release of heavy Ca isotopes from top soils could perhaps also explain the anomalously high $\delta^{44}Ca$ signatures in local groundwater (Fig. 16), as heavy

Ca isotopes liberated during acidic weathering could become accumulated in groundwater Ca pool.

Similar to Ca, a systematic coupling between tau-normalised values and isotope compositions is also observed for Sr, where the acidic and Sr-depleted top soils carry the most radiogenic Sr isotope signatures ($^{87}Sr/^{86}Sr$ of about 0.778), while deeper calcareous and more Sr-rich soils yielded much lower $^{87}Sr/^{86}Sr$ values of about 0.720 to 0.730 (for details see Fig. 17, and data in Table 2).

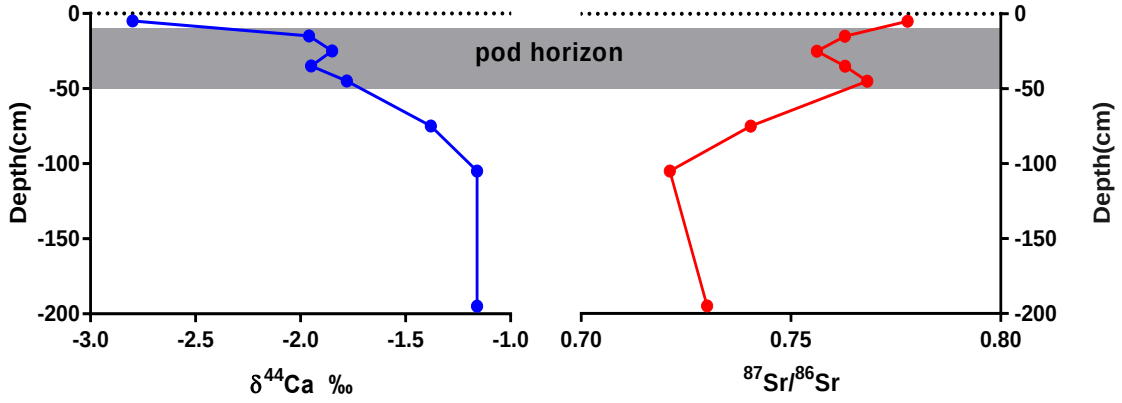

Fig 17. Comparison between Ca and Sr isotope variations in bulk soils, plotted as a function of depth at the studied soil profile at the Lake Chillinup site.

It should be mentioned that one of the most extreme and isotopically light Ca values, with $\delta^{44}Ca$ of up to -4.7‰ (thus almost 2‰ lighter than the top soils) was measured in a sample representing an initial pod formation (see data in Fig. 14 and Table 2). Origin of this extreme Ca isotope anomaly in this young incipient pod is poorly understood, but one could speculate that perhaps upon death of roots and woody tissues, that contain presumably isotopically light Ca-oxalate phase -bound in vacuoles of cells and within organics, this isotopically light and organically-complexed Ca could be released and

pre-concentrated in those initial pod structures(Schmitt et al., 2013). Alternatively, the isotopically light Ca in this incipient pod could be also related to inorganic processes involving isotope fractionation associated with the sorption of Ca on clays and their exchangeable sites (Dontsova, Norton, Johnston, & Bigham, 2004).

5.3 Coupled Ca and Sr isotope constraints on the sources and genesis of clay pods

Combining the stable Ca and radiogenic Sr isotope proxies has the potential to resolve the dilemma of clay pods formation and the relative role of *inorganic* versus *biogenic* processes responsible for the origin of these soil clay structures. Specifically, the radiogenic $^{87}Sr/^{86}Sr$ proxy represents a powerful tracer for mineral and/or inorganic sources, while the stable Ca isotopes are most sensitive to biological processes. Hence, the $\delta^{44}Ca$ could potentially identify the sources of organically complexed Ca in the studied clay pods, and together with $^{87}Sr/^{86}Sr$ data the relative importance of inorganic versus biological processes in clay formation could be constrained. In Fig. 18, we show a cross-plot with $\delta^{44}Ca$ and $^{87}Sr/^{86}Sr$ coordinates and all measured data from samples collected at the Lake Chillinup site, and these include: (i) soil profile, (ii) clay pods, (ii) vegetation (i.e., roots, leaves, wood), and (iv) local water sources (i.e., rain, groundwater and lake water). This multi-proxy $\delta^{44}Ca$ and $^{87}Sr/^{86}Sr$ isotope approach revealed some very important findings relevant not only for the origin of clay pods but also for the sources of waters and nutrients for the growth of local eucalyptus trees.

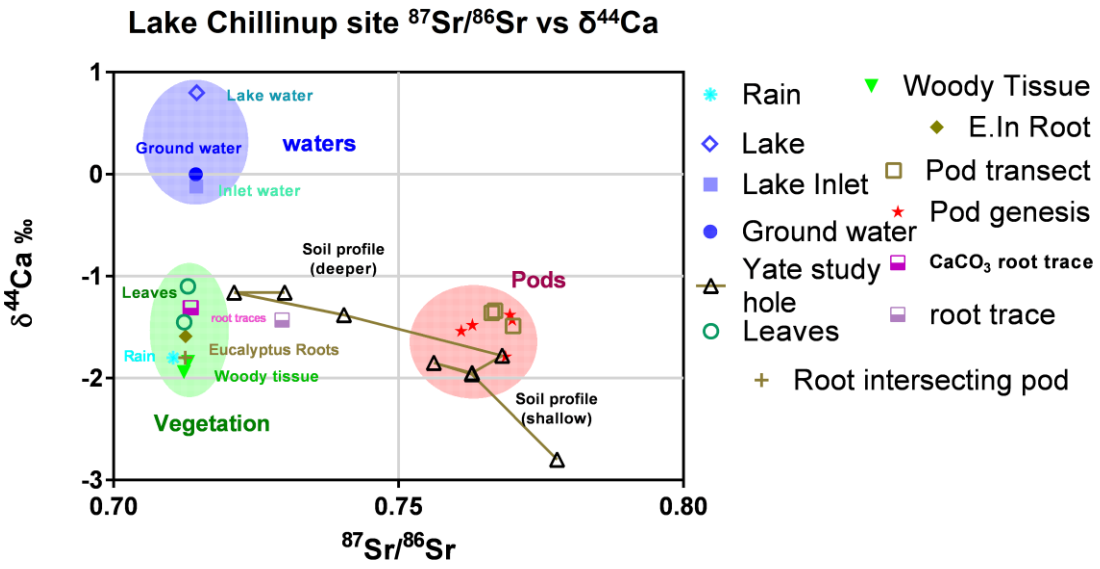

Figure 18: A cross-plot of $\delta^{44}Ca$ and $^{87}Sr/^{86}Sr$ values from Lake Chillinup samples, which include: waters (rain, groundwater and lake waters), vegetation (leaves, roots, wood), soils samples (profile from 0 to 200 cm), and clay pods (including a set of samples representative of pod-genesis process).

Firstly, the Sr and Ca isotope composition of local vegetation (i.e., eucalyptus trees) overlaps with the composition of rain (Fig. 18, see data in green oval), which in turn indicate that the primary sources of alkaline earth metals - and by inference perhaps also other nutrients - for the growth of eucalyptus trees at this site have to be sourced from rainwater and atmospheric deposition, rather then being derived from mineral weathering.

Secondly, the Ca isotope composition of a local groundwater and lake waters is very different and systematically heavier compared to the $\delta^{44}Ca$ signatures found in rain and/or vegetation (see blue and green ovals in Fig. 18). This suggests that eucalyptus trees do not source their waters from the deeper groundwater reservoir and/or nearby lake waters (which are both isotopically very heavy and also saline), but the trees rather utilise perched freshwater sources available at shallower depths, which originated from

a local atmospheric deposition. We speculate that the heavy $\delta^{44}Ca$ signatures found in groundwater and lakes could be related to the removal of light Ca from these pools caused by (i) ongoing precipitation of carbonate minerals in these saline waters, and/or (ii) possible input of isotopically heavy Ca leached from the top soils (Fantle and Tipper, 2014; Farkas et al., 2016), and/or (ii) a combinations of these two processes and some other yet unrecognised factors (i.e., the sorption of light Ca on clays).

Finally, an insight from $\delta^{44}Ca$ and $^{87}Sr/^{86}Sr$ data clearly shows that these alkaline earth metals present in the studied clay pods are not of biological origin and/or sourced directly from local vegetation (i.e., being bio-lifted by eucalyptus trees and excreted via roots at the sites of pods). Our isotope data rather show that Ca and Sr hosted in clay pods have been derived from local mineral soils rather than organic sources and vegetation (see green and red ovals in Fig. 18). This would suggest that material in pods is sequestering from quartz-rich sand dune postulating towards an *inorganic* rather than *biological* genesis.

These findings, however, does not preclude a possibility that other major elements present in clay pods, such as Fe and Al, could be hydraulic lifted by trees and released to the sites of clay formation via roots (i.e., the original phytotarium concept of Verboom and Pate, 2006). However, if correct, this would mean that there has to be an active mechanism for elemental separation by roots of eucalyptus trees, where Ca and Sr are both withheld while Fe and Al are being released by roots into the surrounding soils. Alternatively, and in contrast with the phytotarium concept, the observed enrichments of Fe and Al in clay pods could be related to progressive leaching of these elements from shallow and acidic top soils and their accumulation at deeper depth where the pods are located. Thus, the above *inorganic* versus *biogenic* pathways for the

genesis of clay pods need to be further explored, and the critical parameter to resolve this issue is to constrain the amount of available Fe and Al in the shallow soils, and if these element stocks are sufficient to explain the observed accumulation and enrichments of Fe and Al at deeper depth. A caveat to the above *inorganic* genesis of pods is the nutrient deprived nature of the thin top layer of soil (composed mostly from quartz sand dune material), (Verboom & Pate, 2013). Bulk density analysis of local soils at the Lake Chilliup site is required to infer mass change and elemental fluxes of Fe and Al within each horizon to parameterise the degree of *inorganic* versus *biogenic* emplacement of these elements into clay pod horizons.

5.4 Global perspective on the local ca isotope variability at lake Chillinup

Interestingly, the entire range of $\delta^{44}Ca$ variability measured in samples from the Lake Chillinup site spans about 5.5‰ (i.e., from +0.8‰ for a lake water, up to -4.7‰ for an incipient clay pod). This rather impressive range in $\delta^{44}Ca$ values at our study site is comparable to the entire range of the Ca isotope variability documented in the earth's surface environments on the global scale (see Fig. 19; Fantle and Tipper, 2014). Regardless of such arbitrary comparison between local and global datasets, our data nicely illustrates the complexities of the biogeochemical cycling of Ca in the soil-water-plant system at a local scale, and the potential of $\square^{44}Ca$ proxy for environmental and ecosystem studies, especially if complemented by other and geochemically related isotope tracers such as $^{87}Sr/^{86}Sr$.

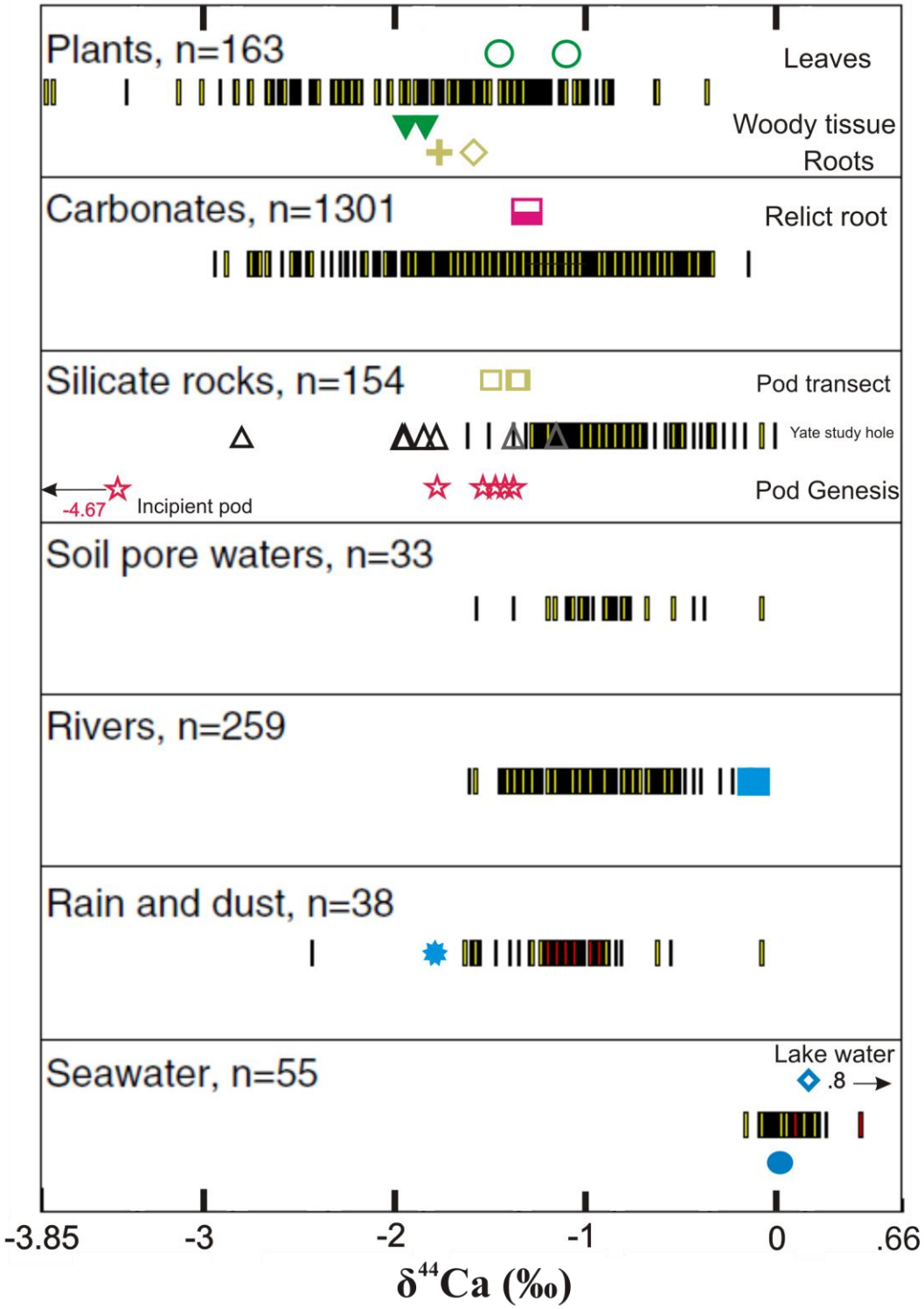

Fig 19. A compilation of Ca isotope data (δ^{44}Ca values relative to IAPSO) documented in various earth's surface reservoirs on a global scale (black symbols = Fantle and Tipper, 2014), plotted along with the δ^{44}Ca variability measured at the Lake Chilliup site, including samples of local vegetation, soils and waters sources (i.e. colour symbols = this study).

6. Conclusions

This study at the lake Chillinup site has uncovered many suggestions regarding local elemental cycles and isotopic differences between local inorganic and organic samples thought to contribute to the genesis of pods under *Eucalypts*. Our findings suggest

- tau normalised profiles within yate soil profile exhibit heavy leaching of transition and alkali metals within topsoil with subsequent enrichments of Al, Fe, Cr, K and Ge within the pod horizon (~10 to 50 cm depth). Sr and Ca concentrations within pod horizon was found to be in trace amounts while both elements were enriched under pod horizons (Max enrichments occurring at ~100 cm depth)
- Such enrichments elicited heavier $\delta\ ^{44}Ca$ signatures suggesting a preferential leaching of the heavy isotope ^{44}Ca thus implicating that Ca-oxolate from roots was not a major component of accumulated Ca.
- Lake and groundwaters exhibited the heaviest signatures likely due to the preference for the lighter ^{40}Ca in biological uptake and precipitation of carbonates thus driving the lake Ca reservoir to heavier signatures.
- Eucalyptus trees carried $^{87}Sr/^{86}Sr$ signatures highly pertaining to local water sources. A close agreement of roots to rainwater signatures suggests that tap roots are sequestering nutrients and water from a perched freshwater reservoir above saline groundwater.
- $^{87}Sr/^{86}Sr$ and $\delta^{44}Ca$ data confirmed that alkali earth metals, such as Ca and Sr, in the studied clay pods originate from the local *inorganic* mineral sources, thus these results do not support the *biogenic* origin of Ca and Sr in pod structures. However, this conclusion may not be directly applicable to the origin of Fe and Al in soil pods, as these major elements are plausibly still be sourced from deeper soils via hydraulic uplift mediated by eucalyptus trees.
- This study contributes the growing database of Ca and Sr isotope measurements from the earth's surface environments and terrestrial ecosystems, with implications for the global Ca and Sr biogeochemical cycles.

ACKNOWLEDGMENTS

Thank you everyone that has helped me this year.

REFERENCES

BARRÉ, P., BERGER, G., & VELDE, B. (2009). How element translocation by plants may stabilize illitic clays in the surface of temperate soils. *Geoderma, 151*(1), 22-30. doi: https://doi.org/10.1016/j.geoderma.2009.03.004

BERNER, E. K., BERNER, R. A., & MOULTON, K. L. (2003). 5.06 - Plants and Mineral Weathering: Present and Past A2 - Holland, Heinrich D. In K. K. Turekian (Ed.), *Treatise on Geochemistry* (pp. 169-188). Oxford: Pergamon.

BOWLER, J. M. (1976). Aridity in Australia: Age, origins and expression in aeolian landforms and sediments. *Earth-Science Reviews, 12*(2), 279-310. doi: https://doi.org/10.1016/0012-8252(76)90008-8

BRANTLEY, S. L., GOLDHABER, M. B., & RAGNARSDOTTIR, K. V. (2007). Crossing Disciplines and Scales to Understand the Critical Zone. *Elements, 3*(5), 307-314. doi: 10.2113/gselements.3.5.307

CHITTLEBOROUGH, T. H. (2017, 12/10/2017). [Chillinup clay is Illite and fine grained Hematite].

DONTSOVA, K. M., NORTON, L. D., JOHNSTON, C. T., & BIGHAM, J. M. (2004). Influence of Exchangeable Cations on Water Adsorption by Soil Clays. *Soil Science Society of America Journal, 68*(4), 1218-1227. doi: 10.2136/sssaj2004.1218

FANTLE, M. S., & TIPPER, E. T. (2014). Calcium isotopes in the global biogeochemical Ca cycle: Implications for development of a Ca isotope proxy. *Earth-Science Reviews, 129*(Supplement C), 148-177. doi: https://doi.org/10.1016/j.earscirev.2013.10.004

FARKAŠ, J., DÉJEANT, A., NOVÁK, M., & JACOBSEN, S. B. (2011). Calcium isotope constraints on the uptake and sources of Ca2+ in a base-poor forest: A new concept of combining stable (δ44/42Ca) and radiogenic (εCa) signals. *Geochimica et Cosmochimica Acta, 75*(22), 7031-7046. doi: https://doi.org/10.1016/j.gca.2011.09.021

FREI, K. M. (2012). Exploring the potential of the strontium isotope tracing system in Denmark. *Danish Journal of Archaeology, 1*(2), 113-122. doi: 10.1080/21662282.2012.760889

GRAUSTEIN, W. C. (1989). 87Sr/86Sr Ratios Measure the Sources and Flow of Strontium in Terrestrial Ecosystems. In P. W. Rundel, J. R. Ehleringer & K. A. Nagy (Eds.), *Stable Isotopes in Ecological Research* (pp. 491-512). New York, NY: Springer New York.

HALVERSON, G. P., DUDÁS, F. Ö., MALOOF, A. C., & BOWRING, S. A. (2007). Evolution of the 87Sr/86Sr composition of Neoproterozoic seawater. *Palaeogeography,*

Palaeoclimatology, Palaeoecology, 256(3), 103-129. doi: https://doi.org/10.1016/j.palaeo.2007.02.028

LUCAS, Y. (2001). The Role of Plants in Controlling Rates and Products of Weathering: Importance of Biological Pumping. *Annual Review of Earth and Planetary Sciences, 29*(1), 135-163. doi: 10.1146/annurev.earth.29.1.135

MARESCHAL, L., TURPAULT, M.-P., BONNAUD, P., & RANGER, J. (2013). Relationship between the weathering of clay minerals and the nitrification rate: a rapid tree species effect. *Biogeochemistry, 112*(1), 293-309. doi: 10.1007/s10533-012-9725-0

PATE, VERBOOM, & GALLOWAY. (2001). Co-occurrence of Proteaceae, laterite and related oligotrophic soils: coincidental associations or causative inter-relationships? *Australian Journal of Botany, 49*(5), 529-560. doi: https://doi.org/10.1071/BT00086

PATE, & VERBOOM, W. H. (2009). Contemporary biogenic formation of clay pavements by eucalypts: further support for the phytotarium concept. *Annals of Botany, 103*(5), 673-685. doi: 10.1093/aob/mcn247

ROMANIELLO, S. J., FIELD, M. P., SMITH, H. B., GORDON, G. W., KIM, M. H., & ANBAR, A. D. (2015). Fully automated chromatographic purification of Sr and Ca for isotopic analysis. *Journal of Analytical Atomic Spectrometry, 30*(9), 1906-1912. doi: 10.1039/C5JA00205B

SCHMITT, A.-D., COBERT, F., BOURGEADE, P., ERTLEN, D., LABOLLE, F., GANGLOFF, S., . . . STILLE, P. (2013). Calcium isotope fractionation during plant growth under a limited nutrient supply. *Geochimica et Cosmochimica Acta, 110*(Supplement C), 70-83. doi: https://doi.org/10.1016/j.gca.2013.02.002

SCHMITT, A.-D., GANGLOFF, S., LABOLLE, F., CHABAUX, F., & STILLE, P. (2017). Calcium biogeochemical cycle at the beech tree-soil solution interface from the Strengbach CZO (NE France): insights from stable Ca and radiogenic Sr isotopes. *Geochimica et Cosmochimica Acta, 213*(Supplement C), 91-109. doi: https://doi.org/10.1016/j.gca.2017.06.039

VERBOOM, W. H., & PATE, J. S. (2006a). Bioengineering of soil profiles in semiarid ecosystems: the 'phytotarium' concept. A review. *Plant and Soil, 289*(1), 71-102. doi: 10.1007/s11104-006-9073-8

VERBOOM, W. H., & PATE, J. S. (2006b). Evidence of active biotic influences in pedogenetic processes. Case studies from semiarid ecosystems of south-west Western Australia. *Plant and Soil, 289*(1), 103-121. doi: 10.1007/s11104-006-9075-6

VERBOOM, W. H., & PATE, J. S. (2013). Exploring the biological dimension to pedogenesis with emphasis on the ecosystems, soils and landscapes of southwestern Australia. *Geoderma, 211–212*, 154-183. doi: http://dx.doi.org/10.1016/j.geoderma.2012.03.030

VERBOOM, W. H., PATE, J. S., & ASPANDIAR, M. (2010). Neoformation of clay in lateral root catchments of mallee eucalypts: a chemical perspective. *Annals of Botany, 105*(1), 23-36. doi: 10.1093/aob/mcp261